Vol. 46, No. 1 (2024) 56-65, DOI: 10.24874/ti.1549.08.23.10

Tribology in Industry

www.tribology.rs

RESEARCH

Experimental Investigations on Wear Phenomena Specific to Rotary Dryer Flights (Blades)

Andrei Burlacu[a], Marius Gabriel Petrescu[a], Răzvan George Rîpeanu[a], Teodor Dumitru[a], Eugen Victor Laudacescu[a,*], Ibrahim Naim Ramadan[a], Adrian Niţă[a]

[a]*Petroleum Gas University of Ploiesti, Romania.*

Keywords:

Flights
Baroid tribometer
Wear granite roller
Wear

* Corresponding author:

Eugen Victor Laudacescu
E-mail: leugen@upg-ploiesti.ro

Received: 13 August 2023
Revised: 14 September 2023
Accepted: 6 October 2023

A B S T R A C T

The experimental research was carried out to study the tribological behaviour of materials used in the manufacture of rotary dryer blades (based on abrasive/abrasive-erosive wear analysis of the blades) using the Baroid tester.

The test program included 2 series of tests consisting of subjecting the specimens to a wear process, generated by friction between their test surface and a rotating granite roller.

Each set of tests was by specific parameters characterized: test medium, rotational speed of the granite roller, pressing force of the roller on the specimen surface, test time, number of test cycles.

The test results highlight the erosion phenomenon (abrasive erosion) responsible for the damage of the rotary dryer blades and the conditions of accentuation of specific wear phenomena.

1. INTRODUCTION

One of the equipment used in the technological process of concrete preparation, subjected to harsh working conditions is the dryer from the concrete plants, with a role in ensuring the mixing of the components that go into the composition the concrete. The service life of the dryer components - especially the mixing arm blades and the armour plating of the mixing tank walls - depends on the size and nature of the aggregates, the degree of acidity of the cement dust, the proportion of sand in the aggregate, etc. [1-5].

The wear mechanism inside a concrete dryer is difficult to control, because the wear of the equipment results from the impact and abrasion of a mixture of particles - some of very small sizes (sand, cement, adhesives) and others of large sizes (the aggregates) - in the presence of water, along with the corrosive wear caused by the acidity of the concrete. Under these conditions, erosion wear, which is specific to the mixture of small particles is accompanied by degradation caused by the impact of large particles on the active elements.

The level of mechanical stress, according to the results of various researchers [6-9], depends mainly on: the hardness of the dryers wetted parts, the impact velocity and the angle of impact.

Concerning the operating behaviour of dryer components, the literature focuses on studying the type and level of mechanical stresses specific to dryer drum and blades, [10-20].

Research in the field has focused on analysing stress states in the drum, including the blades, of dryers as a primary indicator for evaluating abrasive wear due to impact and friction with aggregates, [6,14,20].

Abrasive wear poses a significant challenge in the concrete dryer industry, occurring in both dry and wet conditions. The rotating drums are typically made of steel, and the abrasion resistance of the steel determines the lifetime and mass of the drum. In the study [16] the author designed an experimental stand to test the relative wear resistance of different types of steel under conditions simulating those inside concrete dryers. The tests used crushed granite with dimensions of 16-25 mm and focused on resistance to sliding wear and impact wear for 30 different types of steel, [21].

The experiments described in [21] used a mixture of coarse aggregates and water. The results showed that wear occurs primarily on the external surface, so the materials must ensure wear resistance, as the properties of the interior do not significantly affect the equipment's behaviour.

Regarding the dryer blades, research in the field has focused on studying the effect of aggregate particle size and impact angle on the mechanical stresses to which are the blades subjected.

The paper by Valigi et al. [22] investigates the wear resistance of blades in planetary concrete dryers, and proposes a new blade shape design that improves the dryer's performance. The authors used a combination of experimental testing and numerical simulations to analyse the wear behaviour of different blade geometries and to evaluate the performance of the new design.

The results of the study show that the proposed new blade design significantly reduces wear on the blades compared to the standard blade shape. The authors found that the improved blade shape reduces the formation of cracks and wear patterns, which increases the overall durability of the dryer. Furthermore, the numerical simulations showed good agreement with the experimental results, indicating that the simulation model can accurately predict the wear behaviour of the dryer flights.

The paper by Valigi et al. [23] investigates the wear resistance and efficiency of blades in planetary concrete dryers. The study was by using a new design of flights carried out and comparing its performance with that of a traditional design. The authors used a 3D simulation model to validate the new blade design and evaluate its mixing efficiency. They also conducted laboratory tests to compare the wear resistance of the new and traditional blades. The results showed that the new blade design performed better than the traditional one in terms of wear resistance and mixing efficiency.

The scientific work [24] presents the results of an experimental investigation on a new type of blade for planetary concrete dryers, in order to assess the wear resistance of this new blade design compared to traditional blades. The results of this study suggest that the new designed blade has better wear resistance and this finding is significant as wear is a major issue in concrete mixing, as it can lead to increased maintenance costs and downtime.

The investigation performed in [25] is also regarding the wear of blades in planetary concrete dryers. The authors used a 3D optical scanner to evaluate wear rates and validate a new blade design. Two blade shapes were with the same conditions tested, to compare wear rates and the new design's effectiveness in reducing wear. The worn blades were with a 3D scanner measured to validate the new design. The results showed that the new design has a 3% lower wear rate and better discharge time than the standard blade, making it more efficient overall.

The scientific literature contains limited information on the wear characteristics of concrete dryers, where wear occurs not only on the drum equipped with wear arm or but also on the drum and blades.

The equipment used in the manufacture of concrete on industrial scale is designed to deal with the intense operational loads, mainly represented by the abrasive action of the mineral aggregates (sand and stone with different granulations) and the corrosive action of the mixture of water and cement dust.

The materials used to make the active elements of the equipment are often expensive and the manufacturing technology is specific to these applications. This is also the case for dryers in asphalt plants, whose component parts - in particular, the walls and flights together with the drum on which they are mounted - made of special materials, require special maintenance, with replacement intervals being decisive for scheduling maintenance activities for the entire plant.

The present work aims to provide information on how to choose the materials used in the manufacture of flights, based on their tribological behaviour.

2. MATERIALS AND METHODS

The industrial dryer BENNINGHOVEN ECO 2000, that is the subject of this study, located in the concrete station of the company STRABENBAU LOGISTIC SRL, from Prahova County, according to the manufacturer's technical sheet, it has the following constructive-functional characteristics:

- internal diameter of drum - 2200 mm;
- length of drum - 8000 mm;
- the downward angle of drum inclination - 6 degrees;
- drum mantle thickness - 12 mm;
- number of flights in a transversal section - 16;
- flight sheet thickness - 8 mm;
- the length of the mounting side of flight - 800 mm (mounting detail, according to Figure 1).

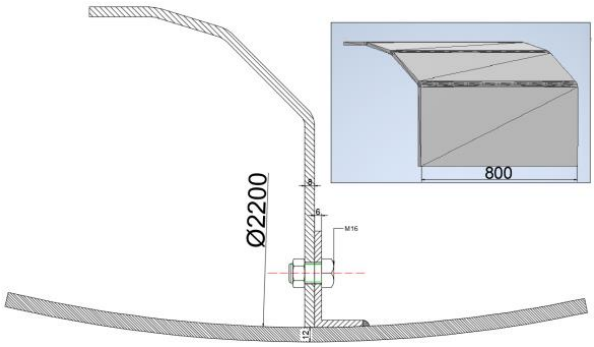

Fig. 1. Mounting detail for flight.

The experimental investigations carried out aimed at studying the tribological behaviour of the used materials in the manufacture of rotary dryer flights (based on abrasive/abrasive-erosive wear analysis of the flights), using the Baroid tester.

The experimental program went through the following course (Figure 2).

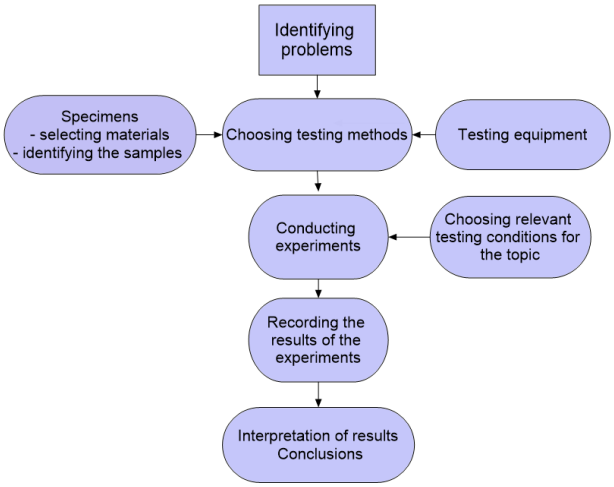

Fig. 2. Research program map.

For the tests, specimens were from a new flight taken (Figure 3), intended for the dryer drum in the asphalt preparation plant.

(a) (b)

Fig. 3. The flights from the drum dispersion zone of dryer, BENNINGHOVEN: (a) top view; (b) side view (traces of specimens sampling can be observed).

The specimens, which were parallelepipedic in shape, had dimensions of 20x20x8 mm. In order to ensure correct attachment to the Baroid tribometer, each specimen was glued to a carbon steel support plate measuring 20x20x4 mm, thus obtaining parallelepiped specimens measuring 20x20x12 mm (Figure 4).

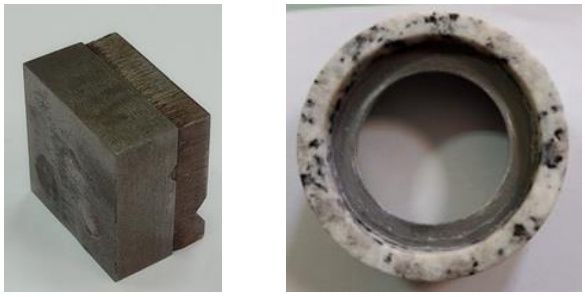

(a) (b)

Fig. 4. Preparing of test specimens (steel) and granite rollers: a - steel specimen, sampled from a flight of the dryer; b - granite roller.

The test programme comprised two sets of tests consisting of subjecting the specimens to a wear process generated by friction between their test surface and a rotating granite roller (Figure 4).

Each set of tests was by specific parameters characterized: test medium, granite roller speed, pressing force of roller on specimen surface, test time, number of test cycles.

The metal specimens were by cutting obtained on the chisel followed by finishing the front surfaces by grinding.

The granite rolls were by the water jet cutting process obtained, on the cutting machine model WUXI YCWJ-380-X1520, existing in the Machine Tools and Chipping Laboratory of the Mechanical Engineering Department of the Faculty of Mechanical and Electrical Engineering, Petroleum and Gas University of Ploiesti. The used cutting speed was 45 - 60 mm/min.

A Baroid Lubricity Tester tribometer (Figure 5) was to investigate the abrasion and erosion resistance characteristics of the used materials, based on the mass loss (gravimetric units - GU) of the tested samples.

(a) (b) (c)

Fig. 5. Tribometer (Baroid Lubricity Tester), (a) the vessel with working environment, (b) friction coupling, (c) actuating lever for obtaining the pressing force.

The operation of the Baroid tester involves the application to the test specimen of a pressing force resulting from the effect of a torque obtained by the lever arm rotating, under the action of a predetermined load. Under these conditions, the specimen will press on the working roller (a consumable made of mineral material similar to the aggregates used in asphalt mixtures) which is in rotation, thus ensuring relative movement between the two components of the torque. The tester provides the conditions for simulating, under accelerated conditions, the abrasion/erosion processes specific to the movement of mineral aggregates over the surface of the dryer flights, the results being in mass units expressed. The experimental research carried out, concerning wear phenomena, aimed at studying the tribological behaviour of the materials used to manufacture the rotary dryer flights (based on abrasive/abrasiv-erosive wear analysis of the flights), using the Baroid tester.

The tester also offers the possibility to measure the friction coefficient (Baroid onctuousness coefficient) between the working roller and the tested sample.

2.1 Metallographic examination of the tested samples

The specimens, initially embedded in epoxy resin, were properly by sanding and polishing processed, and then attacked with metallographic reagents in order to highlight their metallographic structures.

The specimens were analysed with the metallographic microscope microstructures using different magnification scales (x50, x100, x300), microscopic examination of the samples was performed according to SR EN 17639.

Apparatus used for the processing and examination of metallographic structures:

- cutting machine with abrasive disc and automatic control - METACUT A250 model; programmable machine for embedding metallographic samples - ECOPRESS model; machine for grinding and polishing metallographic samples with automatic head - FORCIPOL 2V model (Figure 6);
- optical metallographic microscope - OLYMPUS BX 60M model, equipped with micrometers, eyepiece and objective (for measuring the inclusions dimensions);
- stereoscopic microscope for examination of fracture surfaces - NAMICON model;
- camera on microscopes mounted - OLYMPUS 5050 model.

The metallographic analysis shows ferritic-pearlitic structures, as shown in figure 7.

(a) (b) (c)

Fig. 6. Apparatus used for the processing and examination of metallographic structures, (a) cutting machine with abrasive disc and automatic control - METACUT A250 model, (b) programmable machine for embedding metallographic samples - ECOPRESS model, (c) machine for grinding and polishing metallographic samples with automatic head - FORCIPOL 2V model.

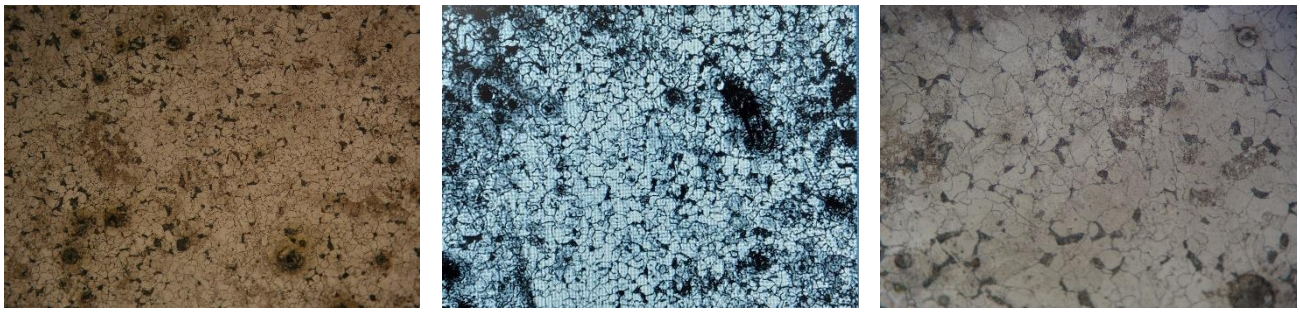

(a) (b) (c)

Fig. 7. Metallographic structure (ferritic-pearlitic), using different magnification scales: (a) x50, (b) x100, (c) x300.

2.2 Hardness Determination

The test was carried out according to SR EN ISO 6507-1:2018 - Metallic materials. Vickers hardness test. Part 1: Test method, and SR EN ISO 6506-1:2015 - Metallic materials. Brinell hardness test. Part 1: Test method, using the Emcotest M4C 025 G3M hardness tester. The test results are in Table 1 presented, and indentation appearance obtained when measuring hardness is in Figure 8 illustrated.

Table 1. Hardness values for tested samples.

Hardness values, HB												Average value, HB
Sample - flight of dryer	149	151	147	152	147	154	148	150	147	150	151	**150**

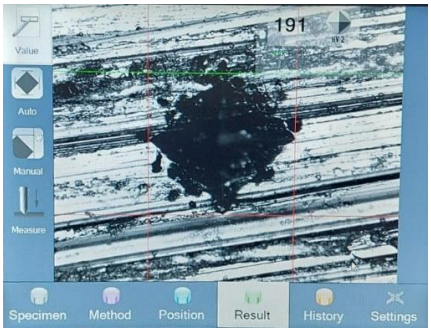

Fig. 8. Indentation appearance obtained when measuring hardness.

2.3 Chemical Composition of the Studied Steel Samples

The material from which the flight is made, that was used in the experimental tests has the chemical composition shown in Table 2. In terms of chemical composition, it is confirmed that the material from which the flight is made is a steel S235JR, according to SR EN 10025:2:2004/AC: 2005.

Table 2. Chemical composition of steel samples

Sample	Chemical composition, %									
	C	Si	Mn	P	S	Cr	Mo	Ni	Nb	V
*Z*1/1 *Z*1/2 *Z*1/3	0,1710	0,0320	1,370	0,0106	0,0032	0,0279	0,0017	0,0205	<0,0005	0,0029

2.4 Determination of microgeometric parameters of steel samples

The research was performed by grinding the surfaces of the specimens on a plane-peripheral grinding machine. To determine the microgeometrical characteristics of the surfaces, the SURTRONIC 3+ profilometer, [26] (Figure 9) was used, and the obtained values were processed using the TalyProfileLite 2.1 program. The parameters can be calculated by referencing the asperity profile (*P*), or after filtering to the roughness profile (*R*), or to the waviness profile (*W*). The filter type and reference length are defined for each parameter, according to the ISO 4287 standard, [27]. Using a Gaussian filter and reference length l_c = 0.8 mm, roughness parameters R_a, R_t, R_z, bearing curves (Abbott-Firestone), and profilograms for the test specimen surfaces were determined.

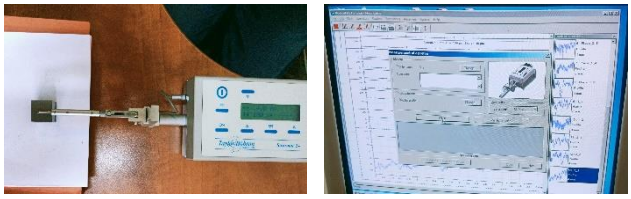

(a) (b)

Fig. 9. The SURTRONIC 3+ type profilometer - the measurement process: a. measurement process; b. image on the monitor.

Table 3 shows the profile parameters of the processed surfaces, the measured roughness parameters, corresponding to the tested samples and Figure 10 shows the profile curves for steel samples, *Z*1/1, *Z*1/2, *Z*1/3.

Table 3. Roughness values of steel samples

Sample	*Z*1/1	*Z*1/2	*Z*1/3
Roughness R_a, µm	1,71	1,794	1,42

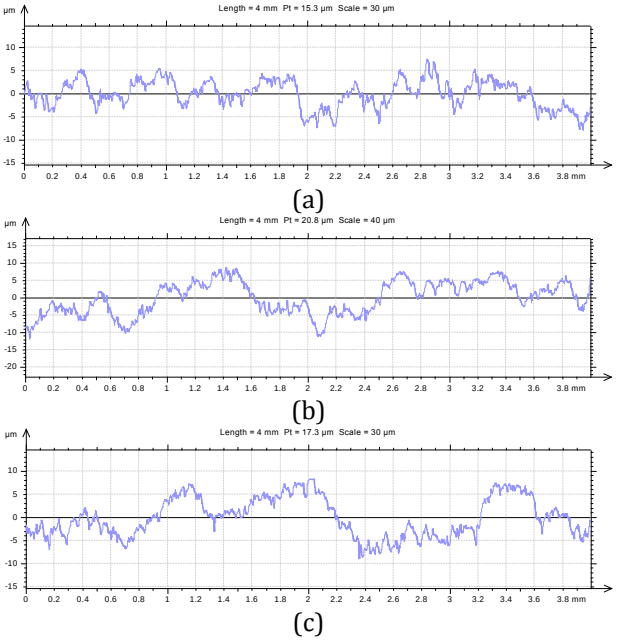

Fig. 10. The profile curves for contact surface of steel samples: a. *Z*1/1; b. *Z*1/2; c. *Z*1/3.

2.5 The rollers material characteristics

The rollers material quality was in accordance with SR EN 1469:2005, SR EN 12057:2005 and SR EN 12058:2005, as it appears from the manufacturer's conformity declaration (SC VIGOMARM SRL).

The rollers were made from calc - alkaline granite - whitish grey, with the following mineral composition: feldspars (55-65%) - light grey crystals of albite and plagioclases; quartz (25%); biotite - muscovite (3-5%); amphibole (5-7%); and opaque mineral elements (1-3%, represented by magnetite and ilmenite), respectively secondary minerals (kaolinite).

The rolls were cut from a semi-finished homogeneous product (a plate of 500 x 500 x 10 mm. The surface was smooth, without bumps or unevenness. No deviations from flatness were found.

The rollers material had the following physical-mechanical characteristics:

- water absorption at atmospheric pressure - 0.38%;
- water absorption by capillarity, mass variation - 0.004 g/m^2.s$^{0.5}$;
- apparent density - 2608 kg/m^3;
- open porosity - 0.52%;
- compressive strength - 186 MPa;
- flexural strength - 15.86 MPa;
- resistance to abrasion (Capone method) - 15.85 mm
- slip resistance: in dry conditions test - 99; in wet conditions test - 92;
- thermal shock resistance – ΔV = 0.01 %; ΔE = 6.97 %.

2.6 The Microgeometrical Parameters Determination

The granite rollers were similarly to the cast iron samples investigated, the results of the roughness measurements being in Table 4 presented and Figure 11 shows the profile, roughness and lift curves for the roller R2.

Table 4. The values of granite rollers roughness.

Rollers symbolization	1	2	3
Roughness value, R_a, µm	5,14	3,06	2,17

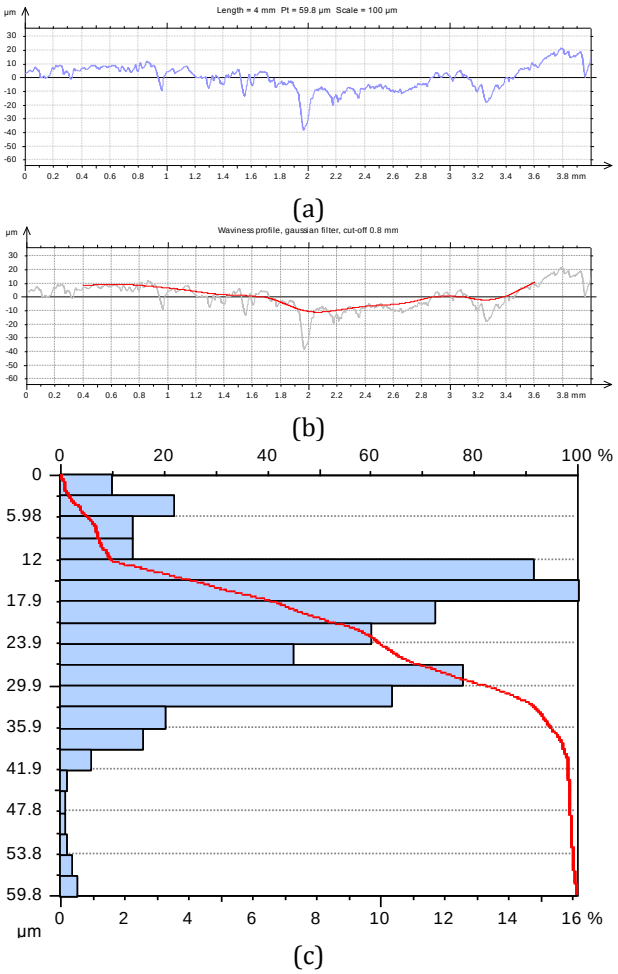

Fig. 11. Profile, roughness and bearing curves for the roller *R*2: a - profilogram; b - profilogram and corrugation; c - the bearing (Abbott-Firestone) curve.

3. RESULTS AND DISCUSSION

The wear of the cast iron samples was determined gravimetrically by weighing at different moments with a KERN ALJ type analytical balance with 10^{-4} g accuracy. For each test the samples were washed with methyl-ethyl-ketone (MEC), wiped with a solvent-resistant microfiber cloth and dried in warm air.

In order to characterize the materials under operating conditions, the experimental program included two sets of tests, using different working environments.

I. The first set of tests was characterized by the following conditions:

- working environment - air;
- rotation speed of the granite roller – n_{roller} = 60 (±5) rot/min;

- pressing force of the roller on the specimen surface - F_p = 85.5 N;
- testing time - t_i = 15 min;
- number of test cycles - 10;
- tested specimens: sample *Z*1/1 with roller 1.

The comparative results of the mass loss measurements (sample mass after each test cycle and cumulative mass loss), for the couple formed by sample *Z*1/1 and roller 1 in air environment, are shown in Table 5 and Figure 12.

Table 5. Results of the first set of wear tests.

Crt. Nr.	Σ t_i, [min]	Sample *Z*1/1 with roller 1	
		m - sample mass, g	*m*, [g]
1	0	37,9282	0
2	15	37,9120	0,0162
3	30	37,9066	0,0216
4	45	37,8999	0,0283
5	60	37,8834	0,0448
6	75	37,8749	0,0533
7	90	37,8669	0,0613
8	105	37,8557	0,0725
9	120	37,8523	0,0759 (Figure13)
10	135	37,8464	0,0818
11	150	37,8348	0,0934

II. The second set of tests was characterized by the following conditions:

- working environment - dry sand (granulation 0 - 4 mm). To maintain similar test conditions, after each test cycle the working environment was restored (fresh sand);
- rotation speed of the granite roller – n_{roller} = 60 (±5) rot/min;
- pressing force of the roller on the specimen surface - F_p = 57 N;
- testing time - t_i = 10 min;
- number of test cycles - 10;
- tested specimens: sample 1/2 with roller 2.

The comparative results of the mass loss measurements (sample mass after each test cycle and cumulative mass loss), for the couple formed by sample *Z*1/2 and roller 2 in dry sand environment, are shown in Table 6 and Figure 12.

Table 6. Results of the second set of wear tests.

Crt. Nr.	Σ t_i, [min]	Sample *Z*1/2 with roller 2	
		m - sample mass, g	Σ Δ*m*, [g]
1	0	37,8351	0
2	10	37,8258	0,0093
3	20	37,8072	0,0279
4	30	37,8019	0,0332
5	40	37,7948	0,0403
6	50	37,7861	0,0490
7	60	37,7810	0,0541
8	70	37,7732	0,0619
9	80	37,7497	0,0854 (Figure 14)
10	90	37,7206	0,1145
11	100	37,7077	0,1274

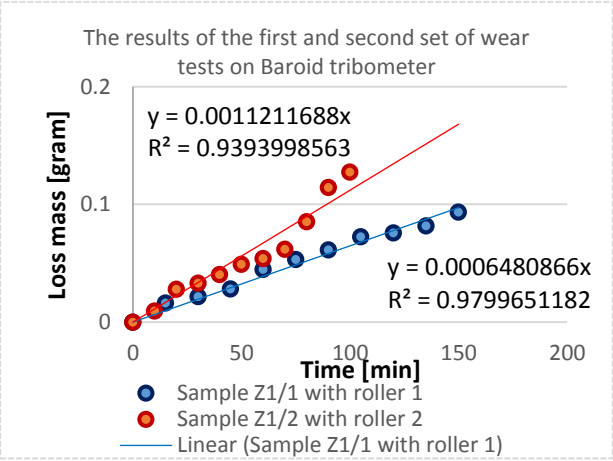

Fig. 12. The results of the second set of wear tests; *R* - Pearson correlation coefficient.

The obtained appearance of the tested surfaces, in terms of the obtained footprint and its image seen under the microscope at 200x magnification, is shown in Figure 13, for the first set of tests and in Figure 14, for the second set of tests.

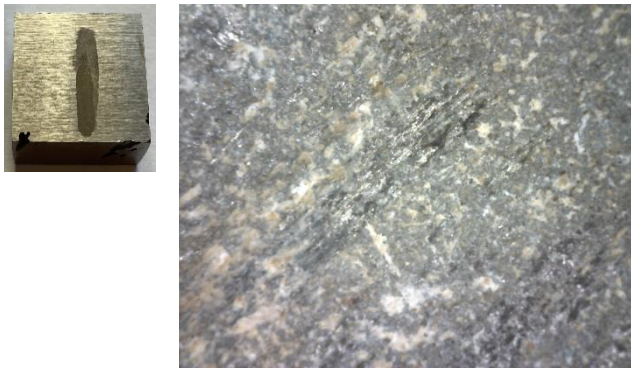

(a) (b)

Fig. 13. Result of the first set of wear tests (example) - sample *Z*1/1 worn, after 120 minutes - 8 operating cycles: a. overall appearance; b. microscopic surface appearance.

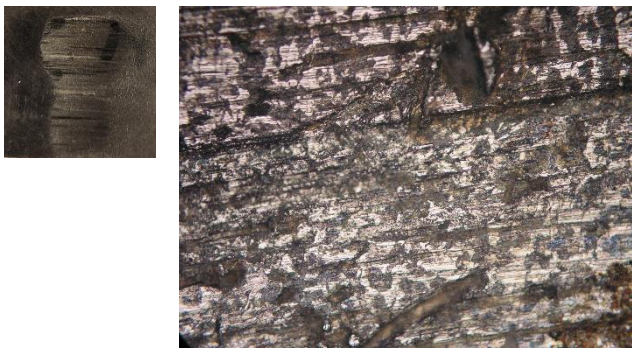

(a) (b)

Fig. 14. Result of the first set of wear tests (example) - sample *Z*1/2 worn, after 80 minutes - 8 operating cycles: a. overall appearance; b. microscopic surface appearance.

4. CONCLUSIONS

Analysing the results of the experimental tests, the following conclusions can be drawn:

- In the presence of dry sand (mineral aggregates), the sample taken from the drying flight shows, as expected, a more pronounced wear than in the test conditions without intermediate medium (sand);
- The presence of sand as an intermediate medium accentuates the abrasion phenomenon, on the sample surface appearing scratches in the direction of the granite roll;
- The presence of sand, in the condition of its entrainment in movement, when rolling the granite roller, accentuates the erosion phenomenon, the surface of the sample being much more affected (obvious pinching) than in the absence of sand.

REFERENCES

[1] B. Cazacliu, "In-mixer measurements for describing mixture evolution during concrete mixing," *Chemical Engineering Research and Design*, vol. 86, no. 12, pp. 1423–1433, Dec. 2008, doi: 10.1016/j.cherd.2008.08.021.

[2] C. F. Ferraris, "Concrete mixing methods and concrete mixers: State of the art," *Journal of Research of the National Institute of Standards and Technology*, vol. 106, no. 2, p. 391, Mar. 2001, doi: 10.6028/jres.106.016.

[3] S. A. Stel'makh *et al.*, "Effects of the geometric parameters of mixer on the mixing process of foam concrete mixture and its energy efficiency," *Applied Sciences*, vol. 10, no. 22, p. 8055, Nov. 2020, doi: 10.3390/app10228055.

[4] M. C. Valigi, S. Logozzo, L. Landi, C. Braccesi, and L. Galletti, "Twin-Shaft mixers' mechanical behavior numerical simulations of the mix and phases," *Machines*, vol. 7, no. 2, p. 39, Jun. 2019, doi: 10.3390/machines7020039.

[5] W. Da Silva Labiapari, R. J. Gonçalves, C. M. De Alcântara, V. Pagani, J. C. Di Cunto, and J. D. B. De Mello, "Understanding abrasion-corrosion to improve concrete mixer drum performance: A laboratory and field approach," *Wear*, vol. 477, p. 203830, Jul. 2021, doi: 10.1016/j.wear.2021.203830.

[6] J. B. Fasano, E. E. Janz, and K. J. Myers, "Design mixers to minimize effects of erosion and corrosion erosion," *International Journal of Chemical Engineering*, vol. 2012, pp. 1–8, Jan. 2012, doi: 10.1155/2012/171838.

[7] S. G. Sapate and A. V. Ramarao, "Effect of erodent particle hardness on velocity exponent in erosion of steels and cast irons," *Materials and Manufacturing Processes*, vol. 18, no. 5, pp. 783–802, Jan. 2003, doi: 10.1081/amp-120024975.

[8] M. Stack, F. H. Stott, and G. C. Wood, "The significance of velocity exponents in identifying erosion-corrosion mechanisms," *Journal De Physique*, vol. 03, no. C9, pp. C9-687 – C9-694, Dec. 1993, doi: 10.1051/jp4:1993972.

[9] Y. A. Khalid and S. M. Sapuan, "Wear analysis of centrifugal slurry pump impellers," *Industrial Lubrication and Tribology*, vol. 59, no. 1, pp. 18–28, Feb. 2007, doi: 10.1108/00368790710723106.

[10] D. M. López, J. P. Congote, J. R. Cano, A. Toro, and A. P. Tschiptschin, "Effect of particle velocity and impact angle on the corrosion–erosion of AISI 304 and AISI 420 stainless steels," *Wear*, vol. 259, no. 1–6, pp. 118–124, Jul. 2005, doi: 10.1016/j.wear.2005.02.032.

[11] C. Braccesi, L. Landi, "An analytical model for force estimation on arms of concrete mixers," *ASME 2009 International Design Engineering Technical Conferences and Computers and Information in Engineering Conference*, vol. 1, pp. 195-204, Jun. 2009, doi:10.1115/DETC2009-86621.

[12] M. C. Valigi and I. Gasperini, "Planetary vertical concrete mixers: Simulation and predicting useful life in steady states and in perturbed conditions," *Simulation Modelling Practice and Theory*, vol. 15, no. 10, pp. 1211–1223, Nov. 2007, doi: 10.1016/j.simpat.2007.07.010.

[13] H. Zhang, F. Pan, and W. Ying, "Abrasive wear and optimal installation angle of concrete double-horizontal shaft mixer stirring blades," *SN Applied Sciences*, vol. 2, no. 6, May 2020, doi: 10.1007/s42452-020-2775-3.

[14] Z. Yao, R. Yang, W. Yuan, H. AN, "Mechanical Analysis and Optimal Design of Mixing Paddles for CSAM Mixers," *Academic journal of manufacturing engineering*, vol. 17, no. 4, 2019.

[15] T. C. Khidir, "Designing, remodeling and analyzing the blades of portable concrete mixture," *International Journal of Mechanical Engineering and Robotics Research*, pp. 674–678, Jan. 2018, doi: 10.18178/ijmerr.7.6.674-678.

[16] A. Burlacu, M. Tănase, C. Ilincă, and M. Petrescu, "Optimizing the trajectory of aggregates in drying units from the asphalt plants," *IOP Conference Series: Materials Science and Engineering*, vol. 1262, no. 1, p. 012003, Oct. 2022, doi: 10.1088/1757-899x/1262/1/012003.

[17] A. Burlacu *et al.*, "Numerical Approach Regarding the Effect of the Flight Shape on the Performance of Rotary Dryers from Asphalt Plants," *Processes*, vol. 10, no. 11, p. 2339, Nov. 2022, doi: 10.3390/pr10112339.

[18] Niță *et al.*, "Experimental research on the wear behavior of materials used in the manufacture of components for cement concrete mixers," *Materials*, vol. 16, no. 6, p. 2326, Mar. 2023, doi: 10.3390/ma16062326.

[19] M. J. Valdes, J. G. A. Marín, M. A. Rodriguez-Cabal, and J. D. Betancur, "Tribometry: How is friction research quantified? A review," *International Journal of Engineering Research and Technology*, vol. 13, no. 10, p. 2596, Oct. 2020, doi: 10.37624/ijert/13.10.2020.2596-2610.

[20] J. C. Silveira, R. M. C. Lima, R. J. Brandão, C. R. Duarte, and M. A. S. Barrozo, "A study of the design and arrangement of flights in a rotary drum," *Powder Technology*, vol. 395, pp. 195–206, Jan. 2022, doi: 10.1016/j.powtec.2021.09.043.

[21] M. Jungedal, "Mild impact wear in a concrete mixer, An evaluation of wet abrasive wear," Ph.D. dissertation, Royal Institute of Technology Department of Material Science and Engineering, SE-100 44 Stockholm, Sweden, 2012.

[22] M. C. Valigi, S. Logozzo, and M. Rinchi, "Wear resistance of blades in planetary concrete mixers. Design of a new improved blade shape and 2D validation," *Tribology International*, vol. 96, pp. 191–201, Apr. 2016, doi: 10.1016/j.triboint.2015.12.020.

[23] M. C. Valigi, S. Logozzo, and M. Rinchi, "Wear resistance of blades in planetary concrete mixers. Part II: 3D validation of a new mixing blade design and efficiency evaluation," *Tribology International*, vol. 103, pp. 37–44, Nov. 2016, doi: 10.1016/j.triboint.2016.06.040.

[24] M.C. Valigi, L. Fabi, I. Gasperini, "Wear resistance of new blade for planetary concrete mixer," *in Proceedings of the 5th World Tribology Congress*, Sep. 2013.

[25] M.C. Valigi, S. Logozzo, I. Gasperini, "Study of wear of planetary concrete mixer blades using a 3D optical scanner," Proceedings of the International Mechanical Engineering Congress & Exposition, vol. 15, Nov. 2015, doi:10.1115/IMECE2015-50632.

[26] S. Dangar, A. Sen, S. Mukherjee, "Optimization of Surface Roughness Parameters through Regression Model Analysis," *International Journal of Engineering Research and Technology*, vol. 3, no. 6, pp. 92-94, Jun. 2014.

[27] Geometrical Product Specifications (GPS) - Surface texture: Profile method - Terms, definitions and surface texture parameters, ISO 4287, 1997.